Journal of Geosciences and Geomatics, 2021, Vol. 9, No. 1, 28-44
Available online at http://pubs.sciepub.com/jgg/9/1/4
Published by Science and Education Publishing
DOI:10.12691/jgg-9-1-4

Biomarker Geochemical Evaluation of Organic Rich Shales in Mamfe Basin, Cameroon

Edwin Ayuk Ndip[1,2,*], Christopher M. Agyingi[1], Matthew E. Nton[2], Michael A. Oladunjoye[2]

[1]Department of Geology, Petroleum Geoscience Research Group at University of Buea, Buea, Cameroon
[2]Department of Geosciences, Pan African University-University of Ibadan, Ibadan, Nigeria
*Corresponding author: ndip.ayuk@ubuea.cm

Received April 02, 2021; Revised May 05, 2021; Accepted May 14, 2021

Abstract The Mamfe Basin is an intra-continental basin in southwestern Cameroon. Shale from Cretaceous strata in the Mamfe Formation has been poorly characterized in terms of their palaeo-environmental conditions and origin of the organic matter. Also, the thermal maturity of the shale has not been well established. The aim of this study is to determine the origin of the organic matter, evaluate the thermal maturity, palaeo-environmental conditions, and thereby deduce their hydrocarbon generative potential. Biomarker geochemical analyses was carried out on the organic matter extracts of some selected shale samples from Mamfe Formation having total organic carbon content ranging from 0.69 and 4.50 wt. % (av. =1.82 wt. %). Base on the total organic carbon content, the shales are described to have good hydrocarbon generative potentials. Thermal maturity parameters base on 20S/(20S +20R), and ββ/(ββ + αα) C_{29} sterane ratios along with CPI and OED indicate that the analysed samples from Mamfe Formation sit at mature oil window generation. The origin of the organic matter have been deduced to be mainly of terrestrial plant source with minor lacustrine and marine influences. Palaeo-environmental conditions were decipher to be of sub-oxic to anoxic conditions that have preserved the organic matter. This study have highlight valuable insight based on the biomarker geochemistry of the shales of the Mamfe Basin thereby reducing petroleum exploration risk.

Keywords: *mamfe formation, shale, organic matter, total organic carbon, biomarker geochemistry*

Cite This Article: Edwin Ayuk Ndip, Christopher M. Agyingi, Matthew E. Nton, and Michael A. Oladunjoye, "Biomarker Geochemical Evaluation of Organic Rich Shales in Mamfe Basin, Cameroon." *Journal of Geosciences and Geomatics*, vol. 9, no. 1 (2021): 28-44. doi: 10.12691/jgg-9-1-4.

1. Introduction

The Mamfe Basin (Figure 1) is an intracontinental basin in Cameroon in which exploration for hydrocarbons is currently ongoing, mostly by some academic researchers. Previous research works indicated that the basin holds potential to generate hydrocarbon gases [1,2] from Cretaceous shale containing type III and IV kerogens [2]. The Mamfe Basin's tectonic history, regional geology, stratigraphy, and sedimentology have been well studied and research publish online by [3,4,5,6]. Important petroleum-exploration questions such as paleodepositional conditions and the thermal maturity for organic matter preserved in the potential source rocks and the origin of the organic matter are yet to be fully answered. Studies on the source rock organic geochemistry of the Mamfe shales to date have been insufficient to describe palaeo-environmental conditions, origin of organic matter, and thermal maturation. Researchers such as [7-12] have widely reported the important of biomarker geochemistry in characterising the source rock's organic matter origin, paleodepositional conditions, and thermal maturation. Therefore, this study employed the used of biomarker geochemistry in order to evaluate the origin of the organic matter, paleodepositional conditions, as well as the thermal maturity of the Lower Cretaceous Mamfe Formation shale.

2. Geological Background

The Mamfe Basin constitutes parts of a series of rift basins in Central and West Africa whose origin is linked to the Cretaceous separation of the African crustal blocks as part of the West and Central African Rift System [13,14,15]. It is bounded to the north and south by the Obudu and Oban massifs, respectively (Figure 1). The Basin narrows eastward, terminating below the Cameroon Volcanic Line (CVL) and opens westward into the Benue Trough across the Cameroon-Nigeria border [13,16]. [17] reported that the Basin is underlain and fringed by reactivated, fault bounded granitic-gneissic rocks of the Pan-African Mobile Belt (550 ± 100 Ma) and is intruded both by Cenozoic orogenic and effusive basic intermediate rocks such as syenites, diorites, and trachytes and by basalts that belong to the CVL. The Mamfe Basin is essentially filled by Cretaceous clastic sedimentary rocks [18], comprising conglomerates, sandstones, arkoses,

black shales, and mudstones [6]. The Lithostratigraphy of the basin was described by [3, 4, 19], and they referred to it as the Mamfe Formation. Several different Lithostratigraphy frameworks have now been published, but, in general, none are accepted. A summary of all the various stratigraphic columns proposed for the Mamfe Basin is documented in [20] and this study uses that of 5 as shown in Table 1.

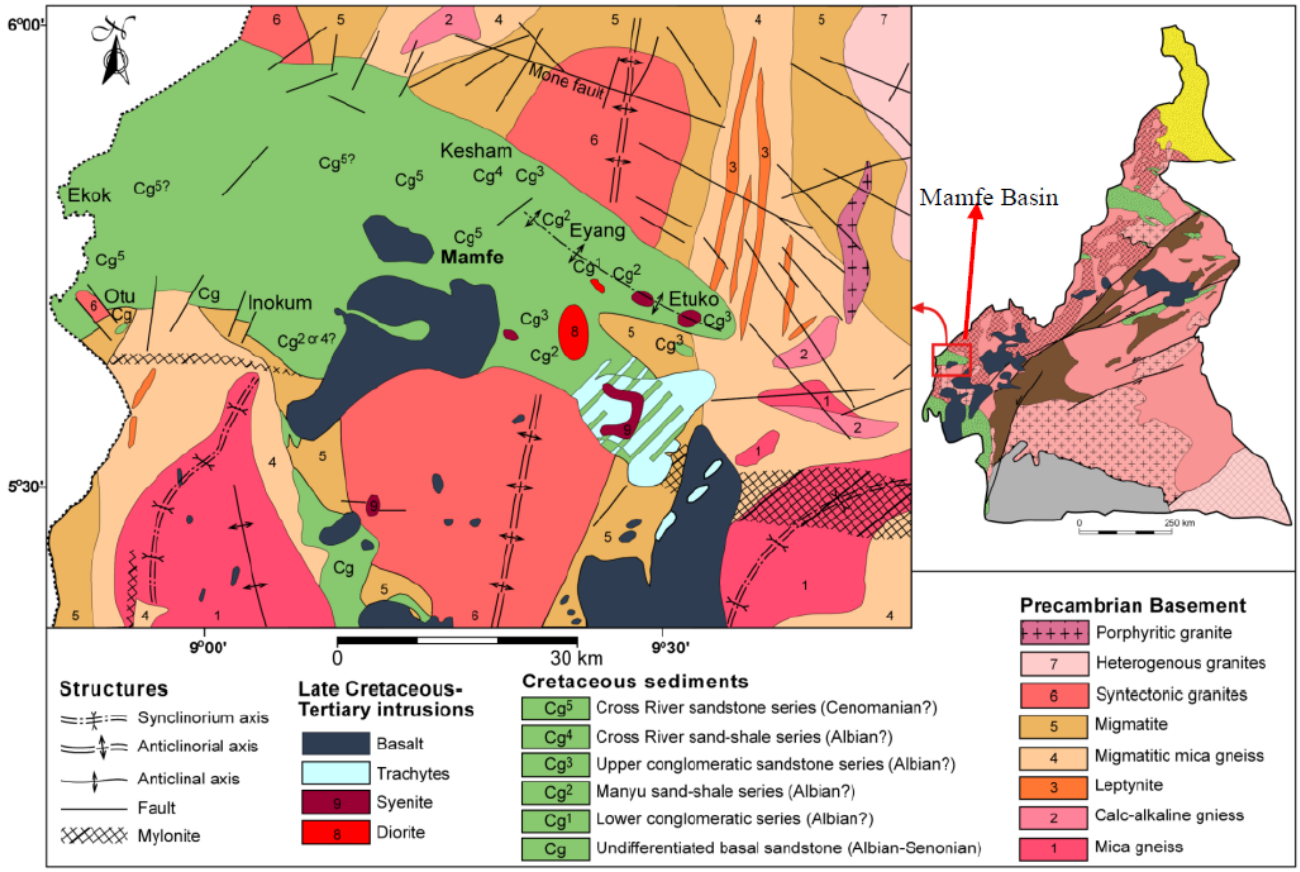

Figure 1. Geologic map of the Mamfe region (modified after 18)

Table 1. Stratigraphy of the Mamfe Basin (after 5)

Age	Formation	Member	Lithologic description
Cenomanian	Mamfe Formation	Manyu	Cross stratified massive to very massive sandstone with mud cracked, shale/ mudstone interbedded.
Albian -Aptian		Nfaitok	Indurated black shale with siltstones interbedded and locally clayey, marlstone and limestone.
Berremian-Aptian		Etoko/Okoyong	Massive sandstone locally with shale interbedded at the top and amalgamated poorly sorted conglomerate with local siltstone beds at base
Pre-Cambrian	Basement	Granitic-gneissic	Granitic - gneissic

3. Methods

Field sampling on exposure in road-cuts and river channels were carried out in the Mamfe Basin. During the field sampling, an attempt was made to collect fresh and un-weathered samples since weathering is a problem in geochemical investigation. A hand driller was used to collect the sample at 1.5-m depth. A total of 16 samples were collected and analysed for total organic carbon content (TOC) using LECO C230 instrument. Only samples with TOC (wt. %) exceeding [21] 0.5 wt. % for source rocks are reported here and used for the biomarker analysis while others were discarded. A pre-weighed portion of powdered 15- 30 g of seven shale samples (with TOC > 0.5 wt. %) was poured into a pre-extracted paper thimble and placed into the soxhlet apparatus. A zeotropic mixture of dichloromethane (DCM) and methanol (CH_3OH) (93:7 v/v, 450 ml) was prepared and placed in a 500-ml round bottom flask. Pre-extracted anti-bumping granule and activated copper tunings were added to the solvent flask which was fitted to the soxhlet extraction. Extraction was allowed to continue for at least 72 hours after which the extract solution was rotary evaporated until only 1-2 ml of solvent remained. The extract was then transferred into a pre-weighed vial and left to dry in air. When dry, the sample and the vial were re-weighed and the extractable organic matter (Bitumen) obtained. The bitumen was then subjected to column chromatography. The column was prepared by packing 400-mm burrettes with silica gel in petroleum ether to about $4/5^{th}$ full. The slurry was topped up with 2-3 spatula of alumina. A 50-mg portion of each rock extract was dissolved in DCM and then transferred onto a dry activated alumina. The mixture of the sample and the alumina was then left open to the air allowing the solvent to evaporate; occasionally the mixture was slightly heated to less than 40°C to

facilitate solvent evaporation. Then the dry adsorbed sample was gently poured into the top column. The rock extracts were separated into saturated hydrocarbons; aromatic hydrocarbons; and Nitrogen-, Sulphur-, and Oxygen-bearing compound. Only the saturated fraction was considered for this study. The saturated fraction was eluted with 80 ml of petroleum ether and the eluate was collected into a labelled 250-ml round bottom flask. The saturated fraction was subjected to Gas chromatography–mass spectrometric (GC–MS) analysis using an Agilent 7890A gas chromatograph coupled with Hewlett-Packard 5975C mass spectrometer. The samples were analysed in the full scan modes and n – alkanes (m/z =85), triterpanes (m/z = 191), and regular steranes (m/z = 217) were detected and individual compound were identified by the relative retention times.

4. Results

4.1. Sedimentology

The outcrops at the various localities of studied are composed of massive to fissile black shales, siltstones, and limestones (Figure 2). Very compact and indurated black shale predominates at the base of the outcrops. The black shales are intercalated with silty shales alternating with siltstones and limestone. Siltstone beds intercalated between the shale are of vary thickness of less than 0.5 cm to about 20 cm and were grey in colour. The limestone beds intercalate between the shales and range in thickness from less than 2 cm to about 20 cm and are grey with no macrofossils in them.

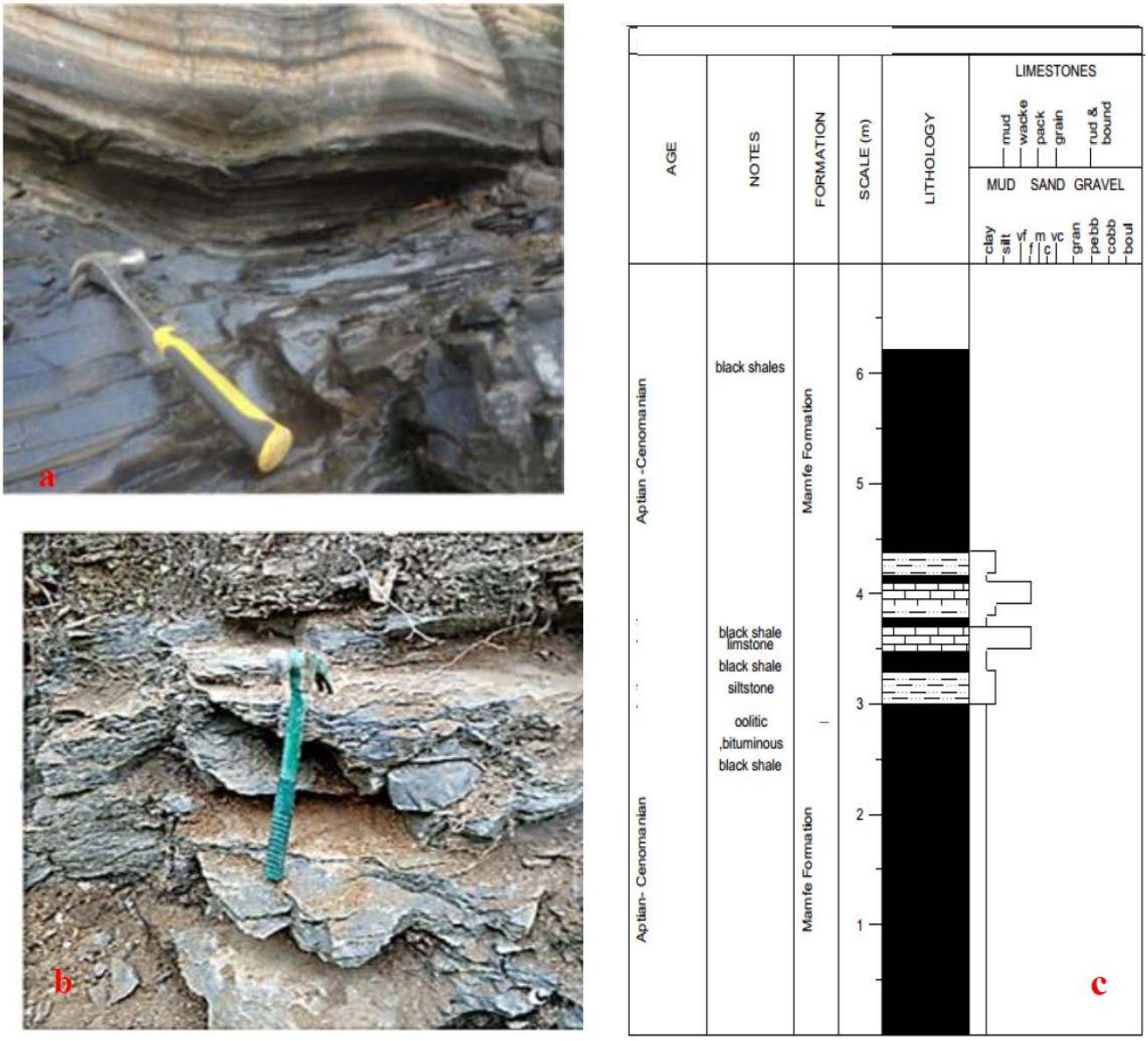

Figure 2. Representatives outcrops (a and b) and lithological log (c) of the Mamfe Formation

4.2. Total Organic Carbon Contents (TOC; wt. %)

TOC content of the analysed samples are shown in Table 2. The percentage of TOC in the studied samples was between 0.69 and 4.50 wt. % (av. =1.82 wt. %), corresponding to good contents of organic matter after [22]. These TOC values do not automatically categorize the samples as potential source rocks because TOC values alone are not sufficient to indicate good source rock

potential because much of the organic matter may be inert due to sedimentary reworking, oxidation, or advanced levels of maturation [23]. However, good preservation of organic matter under anoxic conditions led to the deposition and preservation of these organic matter-rich sediments [24].

Table 2. TOC (wt. %), data calculated from mass chromatograms (*m/z* 85) and derived parameters for the studied samples from Mamfe Formation

Samples ID	TOC (wt. %)	Pr/Ph	Pr/*n*-C_{17}	Ph/*n*-C_{18}	CPI	CPI(1)	OEP(2)	OEP(1)	Waxiness Index	TAR
NM1	1.33	0.72	4.17	1.89	1.30	1.80	1.10	1.32	1.19	47.29
NM2	4.50	1.42	0.63	0.40	0.87	1.09	1.01	0.79	0.48	16.78
NM3	0.69	0.60	2.46	0.65	0.32	1.10	0.85	0.10	0.17	11.12
NM4	2.48	1.71	2.22	2.63	0.74	1.13	1.03	0.67	0.39	18.72
NM5	1.65	1.48	0.23	0.15	0.95	1.09	0.94	0.98	0.47	24.39
NM6	0.70	1.18	0.54	0.43	1.01	1.13	0.96	1.04	0.55	16.11
NM7	1.36	0.96	0.67	0.51	0.92	1.33	0.89	0.65	0.28	13.44

Pr = pristane, Ph = phytane, Pr/Ph = pristane/phytane, Pr/*n*-C_{17}= pristane/*n*-C_{17}, Ph/*n*-C_{18}= phytane/*n*-C_{18},
CPI (carbon preference index) =½[(C_{25} + C_{27} +C_{29} + C_{31} + C_{33}/C_{24} +C_{26}+C_{28}+C_{30}+C_{32}+C_{34}) + (C_{25} + C_{27} +C_{29} + C_{31} +C_{33}/C_{26}+C_{28}+C_{30}+C_{32}+C_{34})],
CPI (1) = 2(C_{23}+C_{25}+C_{27}+C_{29})/[C_{22}+2(C_{24}+C_{26}+C_{28}) +C_{30}],
OEP (improved odd-over-even predominance)
OEP (1) = C_{21}+6C_{23}+C_{25}/ 4(C_{22}+C_{24}),
OEP (2) = C_{25}+6C_{27}+C_{29}/4(C_{26}+C_{28}),
TAR (terrigenous/aquatic ratio) = (C_{27}+C_{29}+C_{31})/ (C_{15}+C_{17}+C_{19}),
Waxiness index =∑ (n-C_{21}-n-C_{31})/∑ (n-C_{15}-n-C_{20}).

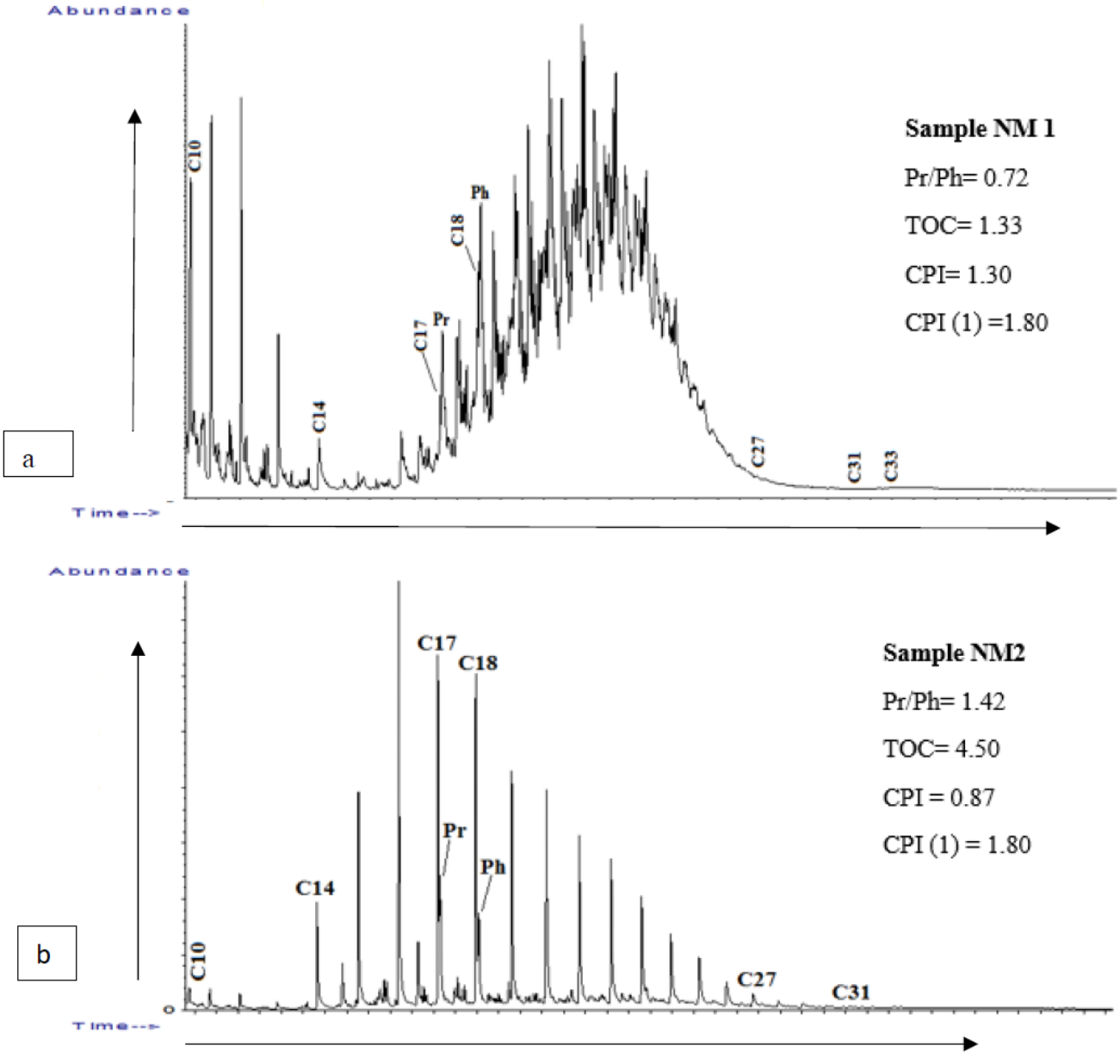

Figure 3a, b. A representative *m/z* 85 mass chromatograms of saturated hydrocarbon fractions of the studied samples

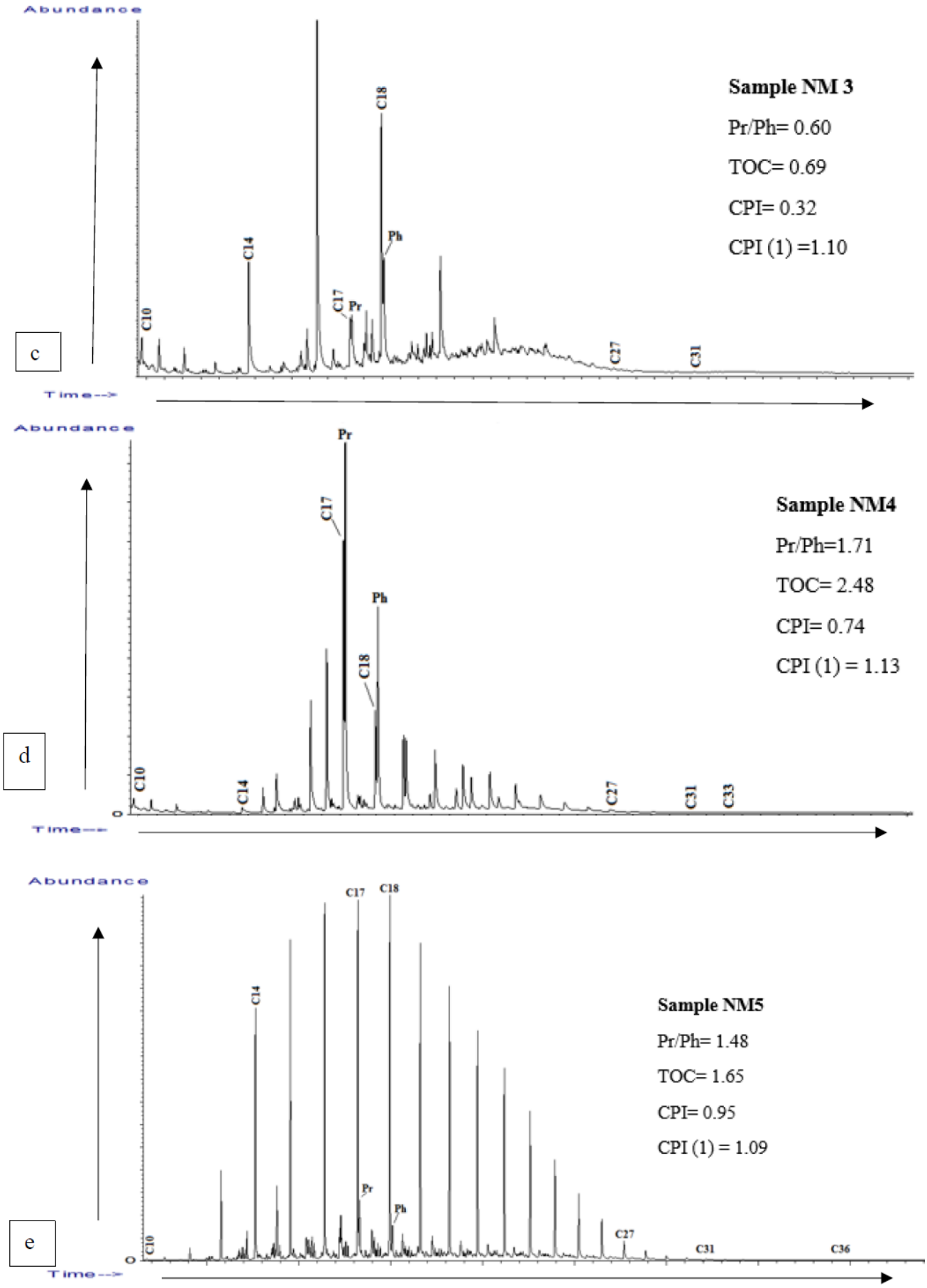

Figure 3c, d, e. A representative *m/z* 85 mass chromatograms of saturated hydrocarbon fractions of the studied samples

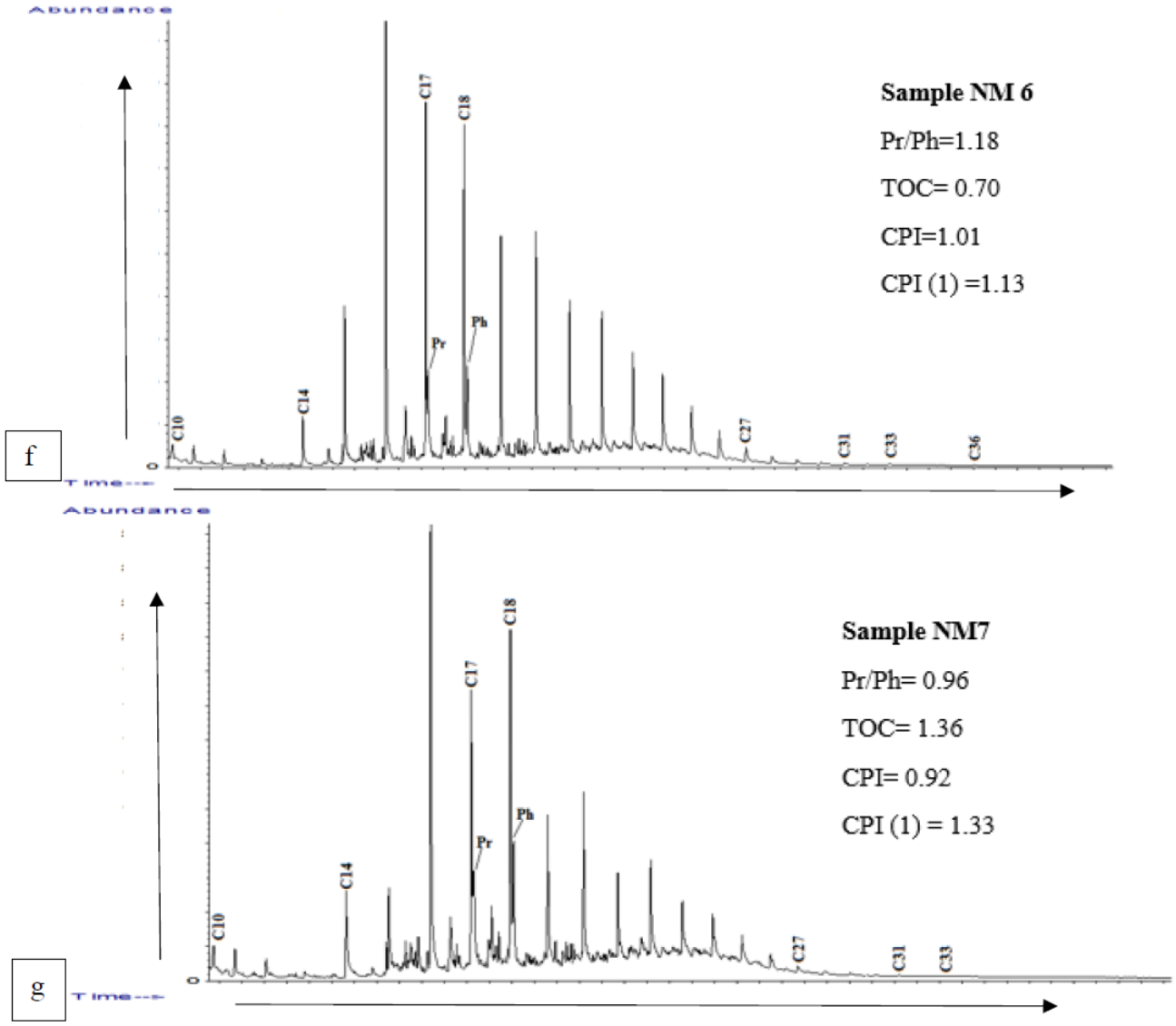

Figure 3 f, g. A representative *m/z* 85 mass chromatograms of saturated hydrocarbon fractions of the studied samples

4.3. *N*-alkane and Acyclic Isoprenoids

The mass chromatograms *m/z* 85 of aliphatic hydrocarbons of the analysed Mamfe samples are shown in Figure 3. The whole-extract gas chromatograms of the Mamfe Formation organic-rich sediments show that *n*-alkanes are the dominant components. The *n*-alkane distributions display a full suite of saturated hydrocarbons C_{10}-C_{36} *n*-alkanes and the isoprenoids pristane and phytane (Figure 3). The Pr/*n*-C_{17} vs. Ph/*n*-C_{18} ratios in the analysed Mamfe samples range from 0.23 to 4.17 and 0.15 to 2.63, respectively, while the Pr/Ph ratios in the analysed samples are in the range of 0.60 to 1.71. The terrigenous /aquatic ratio, TAR = (nC_{27} +nC_{29} +nC_{31}) / (nC_{15} +nC_{17}+nC_{19}) ranges from 11.2 to 47.29. The Waxiness index for the studied samples ranges from 0.28 to 1.19. Lastly, the carbon preference index (CPI; 25, 26, 27) varies between 0.32 and 1.30. The improved odd –even predominance (OEP; 28) values range from 0.65 to 1.32 in the studied samples.

4.4. Terpanes

Triterpane and hopane biomarkers were measured from *m/z* 191 mass chromatograms, respectively (Figure 4). The identified peaks are listed in Table 3 and calculated ratios are in Table 4. The hopanoids biomarkers composition and distribution are relatively the same in the studied samples. The homohopane distributions are characterized by the dominance of C_{31}, and concentrations decrease toward higher-numbered homohopanes (Figure 4) and the C_{31}RHH/C_{30}H hopane ratios of Mamfe extract samples are in the range of 0.002 to 0.17. The C_{29} H/C_{30} H ratios in the studied samples range from 0.42 to 0.57 and are indicating that C_{30}H hopane is in high concentration than C_{29}H – hopane. Other compounds detected include 17β, 21α (H)-moretane, with C_{30}M-moretane/C_{30}H-hopane ratios for the studied samples ranging from 0.18 to 0.27, and 18α (H)-oleanane, with Oleanane index ranging from 0.10 to 0.23. The Ts/ (Ts + Tm) ratios, indicators of thermal maturity, range from 0.33 to 0.63 (Table 4). The Gammacerane index for the extracts varies from 0.07 to 0.23 (av. = 0.09). The ratio of tetracyclic and tricyclic terpanes, represented by C_{24}Tet/C_{26}Tri, range from 0.56 to 1.40 (Table 4) while C_{23}Tri/C_{24}Tet range from 1.10- 9.89. The C_{21}/C_{23} tricyclic terpane ratios also range from 0.12 to 0.84.

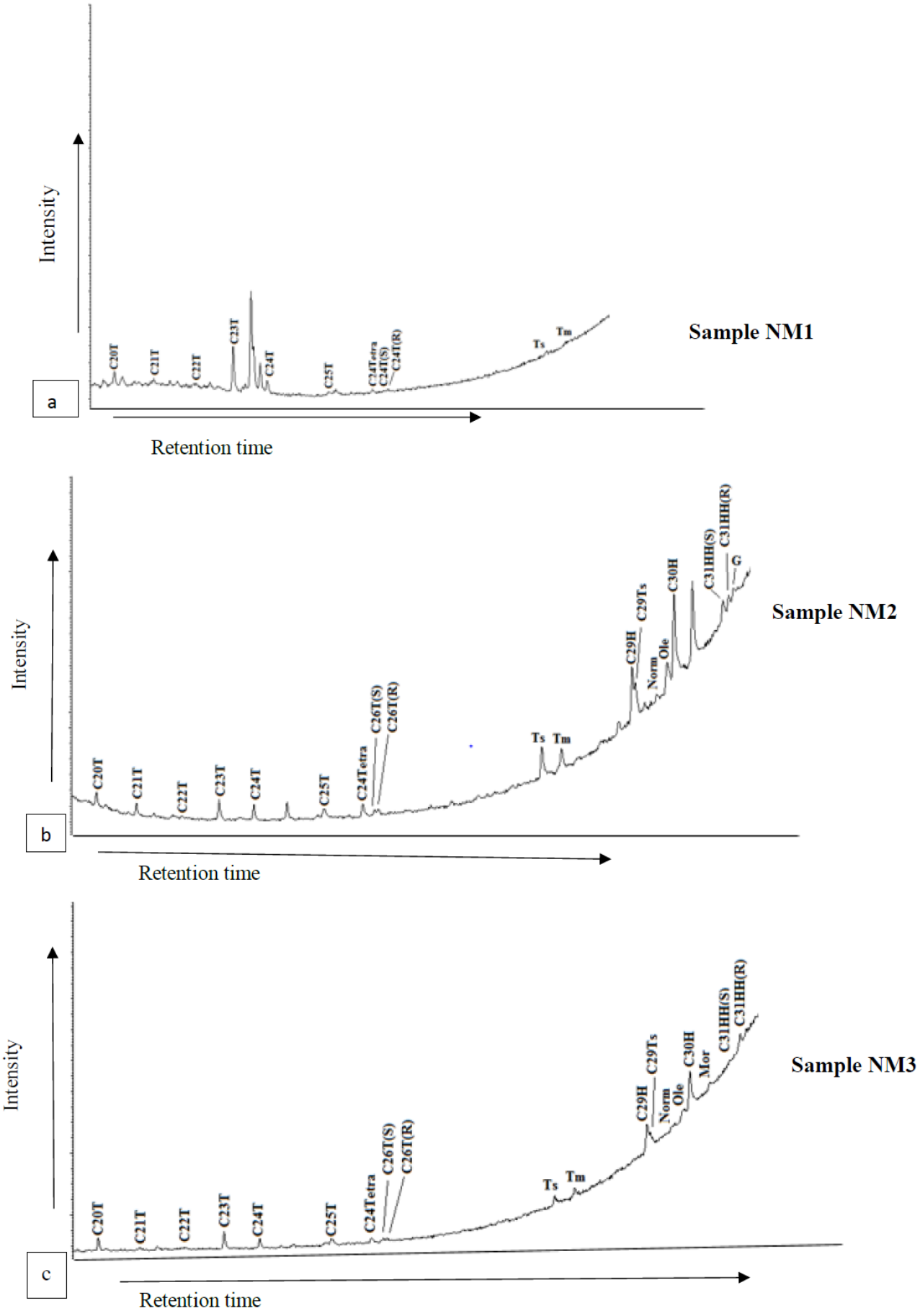

Figure 4 a, b, c. A representative *m/z* 191 mass chromatograms of saturated hydrocarbon fractions of the studied samples

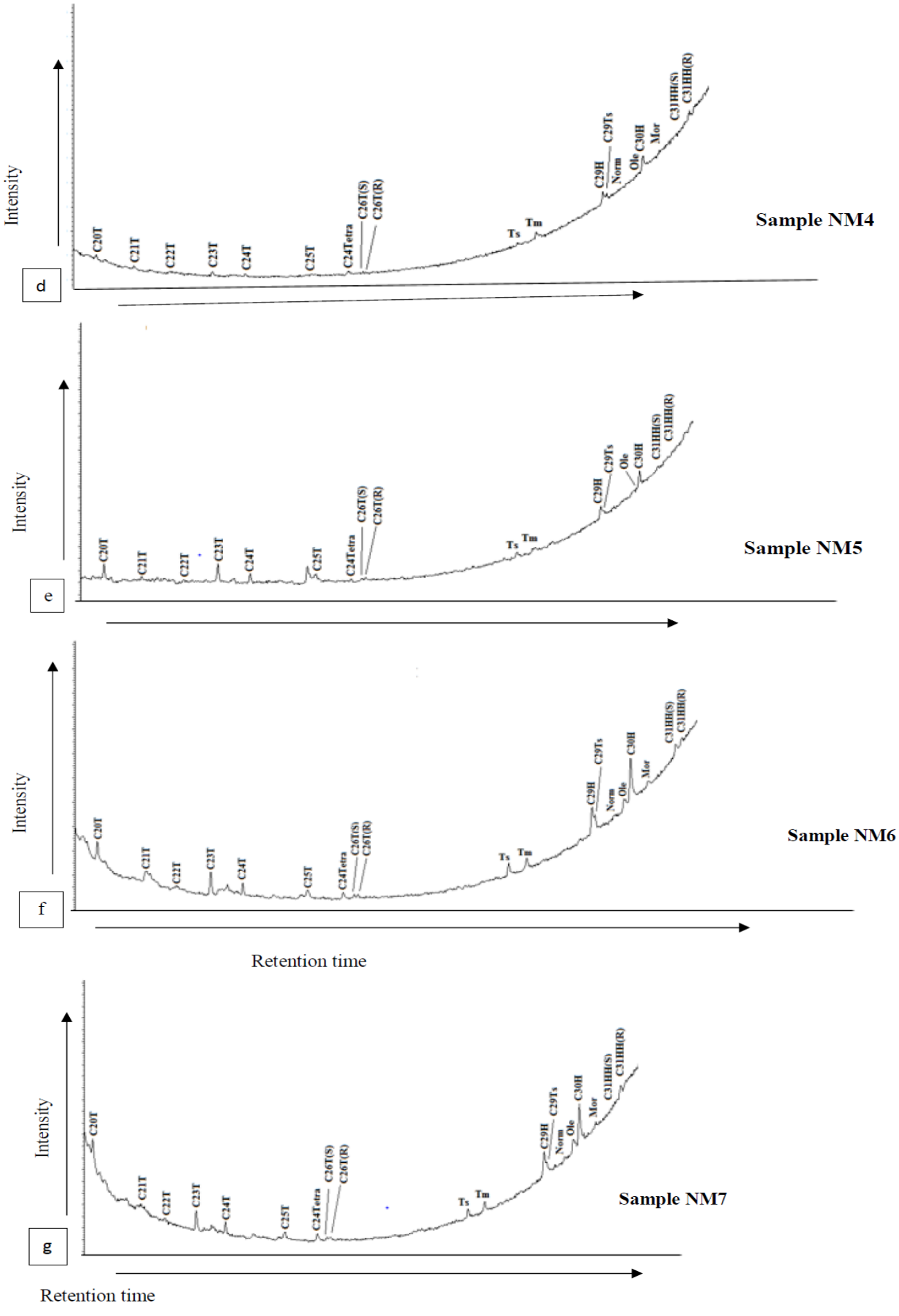

Figure 4 d, e, f, g. A representative *m/z* 191 mass chromatograms of saturated hydrocarbon fractions of the studied samples

Table 3. *m/z* 191 peak assignments for triterpanes in gas chromatograms of saturate fractions

Peak	Compounds
$C_{19}T$	C_{19} tricyclic terpanes
$C_{20}T$	C_{20} tricyclic terpanes
$C_{21}T$	C_{21} tricyclic terpanes
$C_{22}T$	C_{22} tricyclic terpanes
$C_{23}T$	C_{23} tricyclic terpanes
$C_{24}T$	C_{24} tricyclic terpanes
$C_{25}T$	C_{25} tricyclic terpanes
C_{24}tetra	C_{24} tetracyclic terpanes
$C_{26}T$	C_{26} tricyclic terpanes
Ts	18α(H)-22,29,30-trisnorneohopane Ts, C_{29}
Tm	17α(H)-22,29,30 Trisnorhopane Tm, C_{27}
$C_{29}H$	17α(H), 21β(H)-30- norpane C_{29}
$C_{30}H$	17α(H), 21β(H)-hopane C_{30}
C_{31}HHS	22S 17α (H), 21β(H)- 30-homohopane C_{31}
C_{31}HHR	22R 17α (H) ,21β(H)-30-homohopane C_{31}
C_{32}HHS	22S 17α (H) ,21β (H)-30,31-bishomohopane C_{32}
C_{32}HHR	22R 17α(H), 21β(H)-30,31-bishomohopane C_{32}
C_{33}HHS	22S 17α(H) 21β(H)-30,31,32-trishomohopaneC_{33}
C_{33}HHR	22R 17α(H),21β(H)-30,31,32-trishomohopaneC_{33}
C_{34}HHS	22S 17α (H) ,21β (H)-30,31-bishomohopane C_{34}
C_{34}HHR	22R 17α(H), 21β(H)-30,31-bishomohopane C_{34}
C_{35}HHS	22S 17α(H) 21β(H)-30,31,32-trishomohopaneC_{35}
C_{35}HHR	22R 17α(H),21β(H)-30,31,32-trishomohopaneC_{35} Norm Normoretane Ole Oleanane Mor Moretane

Table 4. Biomarker ratios used to assess source rock organic matter origin, paleodepositional environment, and thermal maturity based on terpanes parameters calculated from *m/z* 191 mass chromatograms of the analysed samples

Samples ID	NM1	NM2	NM3	NM4	NM5	NM6	NM7
$C_{29}H/C_{30}H$	-	0.43	0.52	0.57	0.48	0.42	0.43
$C_{31}RHH/C_{30}H$	-	0.16	0.17	0.005	0.004	0.002	0.002
G/31RHH	-	89.47	27.75	40.85	31.74	39.08	-
$G/(G+C_{30}H)$	-	0.09	0.07	0.18	0.12	0.07	-
Ts/Tm	1.37	1.70	1.74	0.5	1.34	1.05	0.98
M/H	-	-	0.19	0.27	-	0.16	0.18
H/(H+M)	-	1	0.84	0.79	-	0.87	0.85
$C_{31}HH$ (S/S+R)	-	0.57	0.68	0.71	0.57	0.64	0.71
$Ga/C_{30}H$	-	0.09	0.08	0.23	0.14	0.07	-
$Ol/(Ol+C_{30}H)$	-	0.22	0.10	0.14	0.18	0.19	0.23
Ts/(Ts+Tm)	0.58	0.63	0.54	0.33	0.57	0.51	0.49
$C_{23}T/C_{24}T$	4.05	1.32	1.71	1.87	1.79	1.88	1.42
$C_{23}T/C_{24}$Tet	9.89	1.63	3.69	1.10	1.79	3.47	2.49
$C_{21}T/C_{23}T$	0.15	0.61	0.23	0.84	0.26	0.12	0.49
$C_{22}T/C_{21}T$	0.75	0.23	0.86	0.31	0.6	2.17	0.5
$C_{24}T/C_{23}T$	0.25	0.76	0.58	0.53	0.56	0.54	0.70
$C_{24}Te/C_{26}$(R+S)tri	1.17	1.73	0.89	1.11	0.56	0.88	1.40
$C_{20}T/C_{23}T$	0.30	0.64	0.73	1.21	0.88	0.96	1.17
C_{26}(R+S)/C_{25} T	0.77	0.66	0.9	1.94	0.89	1	0.68
$C_{29}Ts/C_{29}H$	-	0.29	0.21	0.53	0.28	0.38	0.17
$C_{31}R/C_{30}H$	-	0.16	0.17	0.23	0.22	0.14	0.11
C_{24}Tet/C_{26}(R+S)tri	1.17	1.73	0.89	1.11	0.56	0.88	1.40

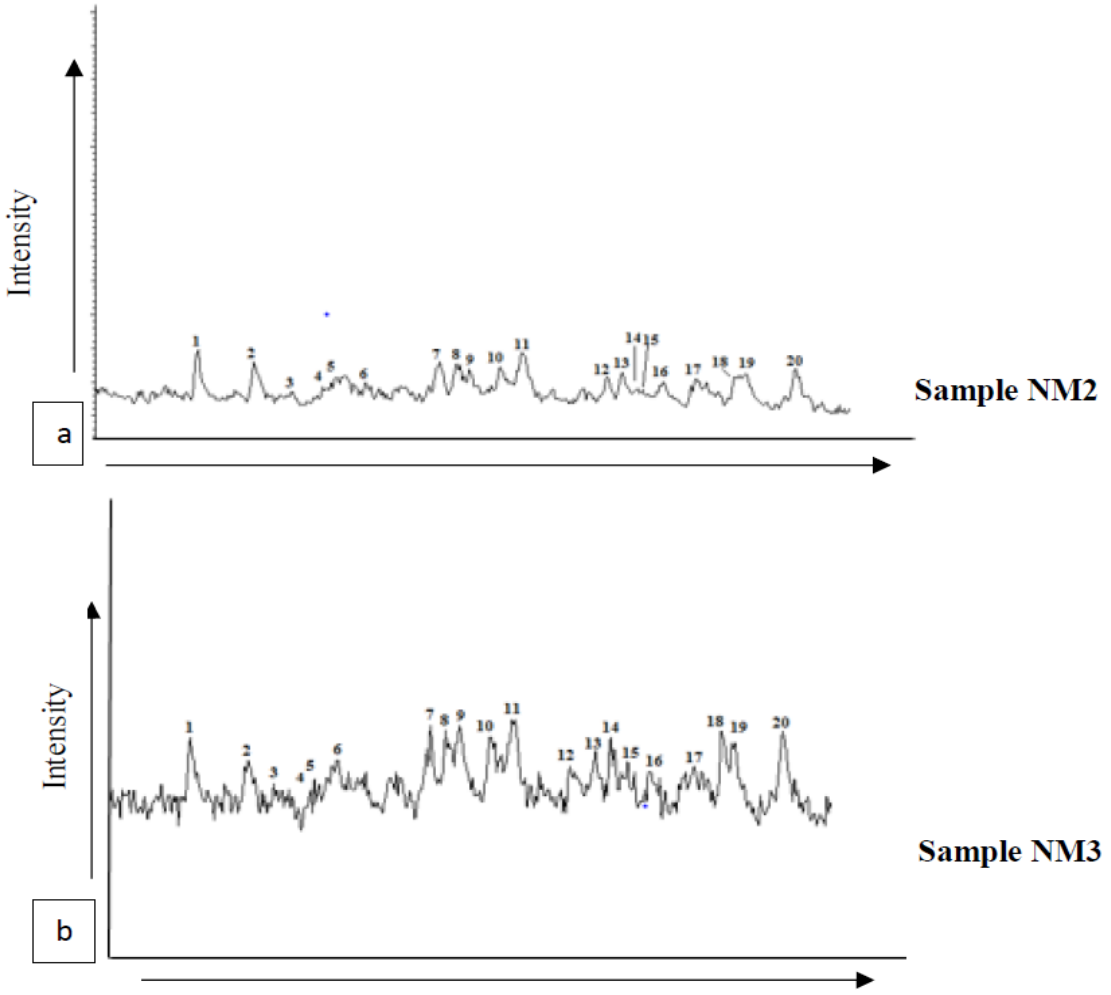

Figure 5 a, b. A representative *m/z* 217 mass chromatograms of saturated hydrocarbon fractions of the studied samples

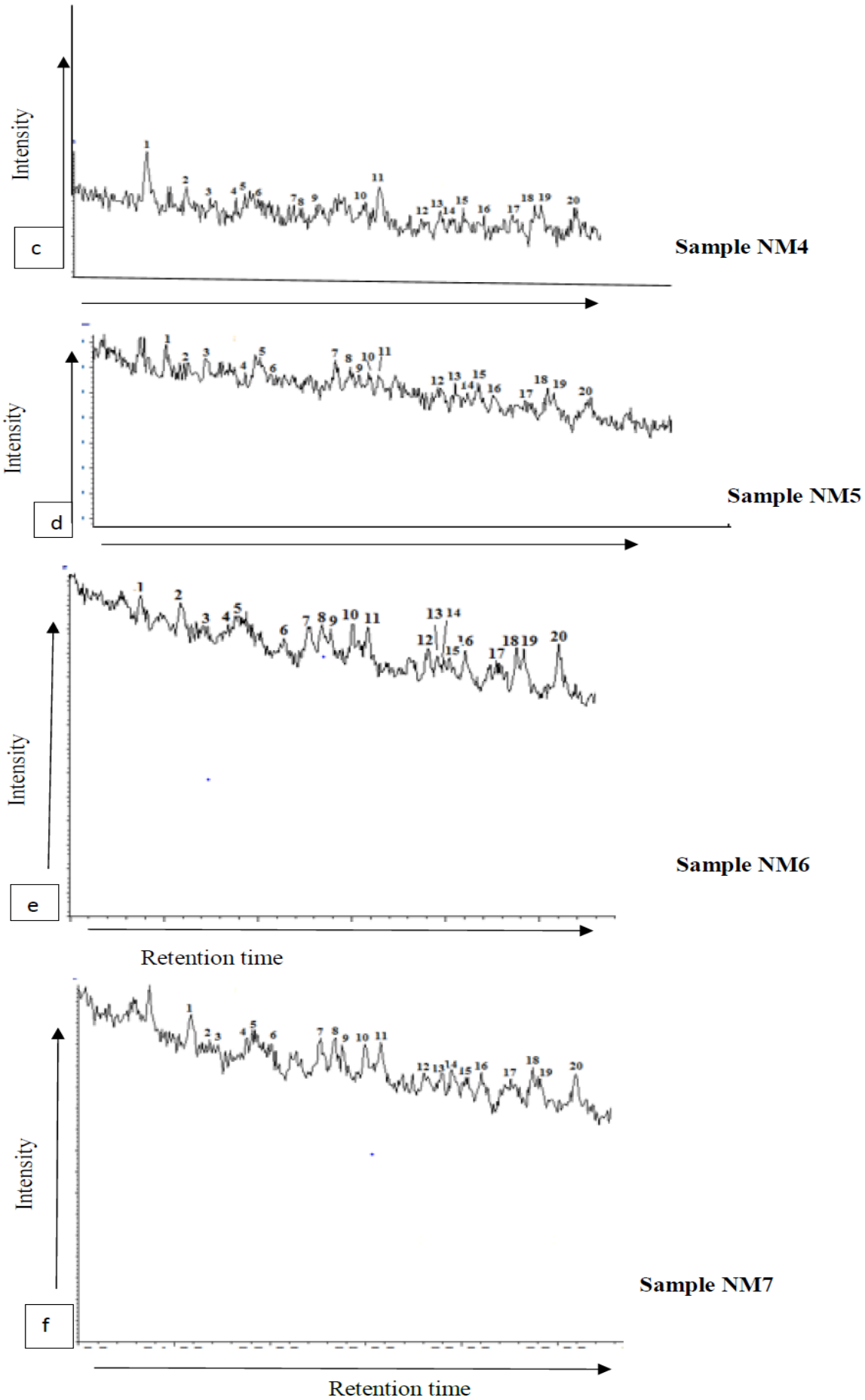

Figure 5 c, d, e, f. A representative *m/z* 217 mass chromatograms of saturated hydrocarbon fractions of the studied samples

Table 5. *m/z* 217 peak assignments for sterane hydrocarbons in gas chromatograms of saturate fractions

Peak	Compounds
1	20S 13β, 17α-diacholestane C_{27}
2	20R 13β, 17α-diacholestane C_{27}
3	20S 13α,17β-diacholestane C_{27}
4	20S 24-methyl-13β,17α-diacholestane C_{28}
5	20R 24-methyl-13β,17α-diacholestane C_{28}
6	20R 24 methyl -13β,17α-diacholestane C_{28}
7	20R 24 methyl -13α,17β-diacholestane C_{28} + 20S 14α,17α cholestane C_{27}
8	20S 24 ethyl -13β,17α-diacholestane C_{29} + 20R 14β,17β cholestane C_{27}
9	20R 24 methyl -13α,17β-diacholestane C_{28} + 20S 14β,17β cholestane C_{27}
10	20R 14α,17α-cholestane C_{27}
11	20R 24-ethyl-13β,17α-diacholestane C_{29}
12	20S 24-ethyl-13α,17β-diacholestane C_{29}
13	20S 24-methyl-14α,17α-cholestane C_{28}
14	20R 24-ethyl-13α, 17β-diacholestane C_{29}+ 20R 24-methyl-14β,17β-cholestane C_{28}
15	24-methyl-14α,17α-cholestane C_{28}
16	20R 24-methyl-14α,17α-cholestane C_{28}
17	20S 24-ethyl-14α,17β-cholestane C_{29}
18	20R 24-ethyl-14β,17α-cholestane C_{29}
19	20S 24-ethyl-14β,17β-cholestane C_{29}
20	20R 24-ethyl-14α,17α-cholestane C_{29}

Tables 6. Sterane biomarker parameters (calculated from *m/z* 217 fragmentograms) of the analysed samples

Samples ID		Ster-C2920S/(20S+20R)	Ster-C29ββ/(ββ+αα)	C_{27}-Ster (%)	C_{28}-Ster (%)	C_{29}-Ster (%)	Ster-C_{27}/Ster-(C_{27}+C_{29})	Ster-C_{29}/Ster-C_{27}	Ster-C_{28}/Ster-C_{29}	S/H
NM1	Mamfe Formation	-	-	-	-	-	-	-	-	-
NM2		0.38	0.18	39.00	29.00	32.00	0.55	0.82	0.92	0.16
NM3		0.30	0.45	35.00	29.00	36.00	0.49	1.02	0.81	0.23
NM4		0.44	0.47	31.00	33.00	36.00	0.46	1.15	0.93	0.28
NM5		0.36	0.41	32.00	33.00	35.00	0.48	1.09	0.95	-
NM6		0.35	0.42	30.00	27.00	43.00	0.41	1.42	0.63	0.23
NM7		0.43	0.38	37.00	29.00	34.00	0.53	0.90	0.88	0.28

4.5. Steranes

Steranes were measured from *m/z* 217 mass chromatograms, which display abundances of "regular" (C_{27}, C_{28}, and C_{29}) steranes (Figure 5). The identified peaks and calculated ratios are presented in Table 5 and Table 6 respectively.

The studied samples have concertation of C_{27}, C_{28}, and C_{29} –steranes that range from 30.00-39.00%, 27.00-33.00%, and 32.00- 43.00%, respectively. The sterane/hopane (S/H) ratio ranged from 0.16-0.28. Other parameters calculated from the *m/z* 217 fingerprints are the C_{29} ββ/ (ββ + αα) and the 20S/ (20S + 20R) for C_{29}steranes. The values of ββ/(ββ + αα) and 20S/ (20S + 20R) for the analysed Mamfe sediments range between 0.18 and 0.47 and 0.30 to 0.44, respectively.

5. Discussions

5.1. Origin of Organic Matter and Paleoenvironmental Conditions

[8,9,12,29,30] have reported that biomarker ratios can provide reliable interpretation of the origin of source rock organic matter (whether it be terrigenous, lacustrine, marine, or mixed source) and conditions of the depositional environment of the organic matter. The *n*-alkanes distributions of the studied samples show a predominance of the low to medium molecular weight compounds (Figure 3). According to [7,31,32] these distributions are typical of terrigenous sediments receiving mixed algal and lacustrine organic matter input. The redox conditions of the source rock depositional environments were interpreted from the pristane/phytane (Pr/Ph) ratios after [7,8,33,34]. It was determined that the Mamfe shale were deposited under relatively reducing depositional environments. However, 35 and 36 note that Pr/Ph ratios can be influenced by source organic materials and also by thermal maturity.

The CPI values for the studied samples indicate a mixed input of marine and terrigenous organic matter deposited under relatively reducing conditions. The cross plot of CPI against Pr/Ph (Figure 6) as well as the cross-plot of the relationship between isoprenoids and *n*-alkanes (pristane/*n*-C_{17} vs. phytane/n-C_{18}; Figure 7) further supports this interpretation. The high TAR values and the waxiness index of the studied samples and the abundance of vitrinite and inertinite macerals in the organic matter of the studied samples, as reported by (2), give credence to a dominance of land plant-derived organic materials. The homohopane distribution in the studied samples indicate a clay-rich character [37,38] and supports the field study done by [6] in the basin.

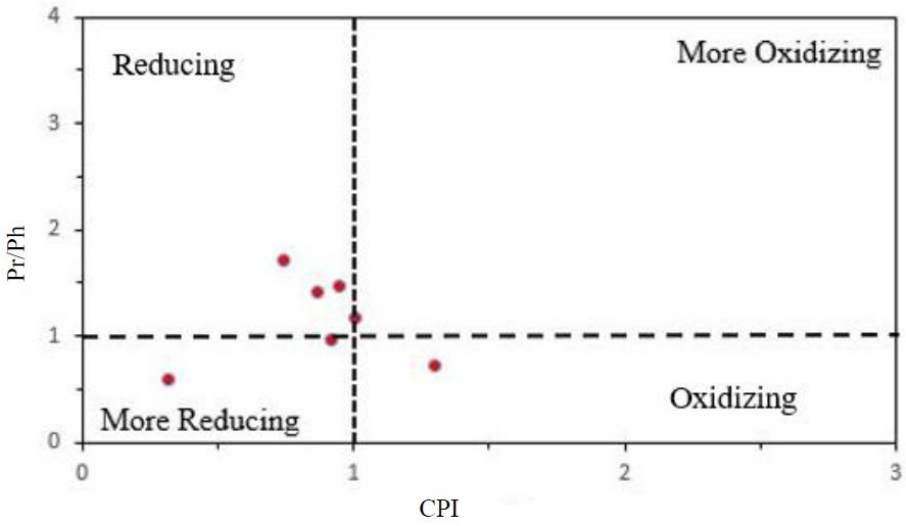

Figure 6. Pr/Ph vs. CPI, indicating paleodepositional conditions of the studied samples (after 27)

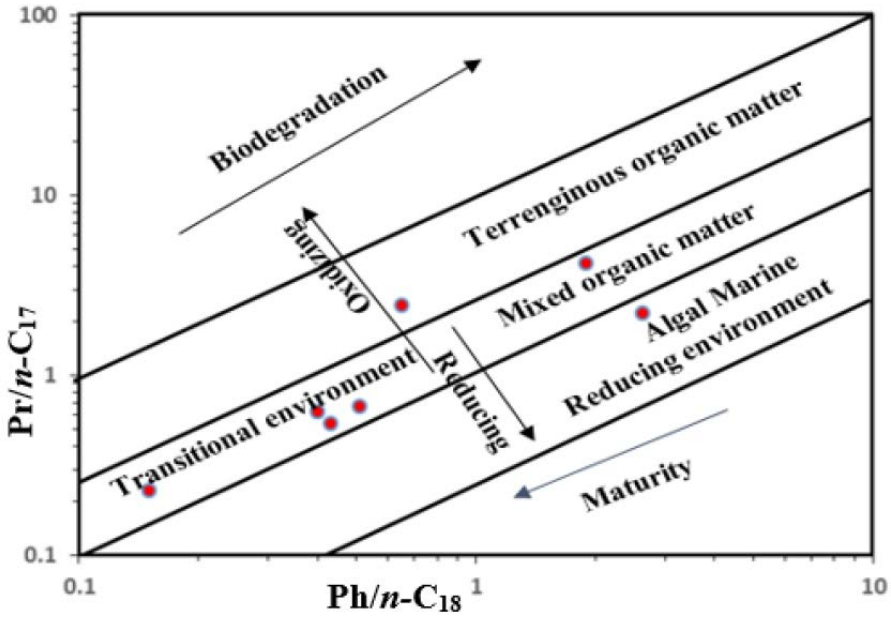

Figure 7. Pristane/*n*-C17 vs. phytane/*n*-C18 for the investigated samples (after 8)

[8] distinguished between marine and lacustrine environment using the C_{31}-22R-hopane/C_{30}-hopane ratio. They indicated that the C_{31}-RHH-hopane/C_{30}-hopane ratio generally higher than 0.25 is for marine environments, whereas the ratio is lower than 0.25 is for lacustrine settings. The C_{31} 22RH/C_{30}H hopane ratios of Mamfe extract samples are indicating a lacustrine environment. Furthermore, the aliphatic isoprenoids Pr/Ph ratios in combination with low hopane biomarker ratios (C_{31}-22R-hopane/C_{30}-hopane vs. Pr/Ph ratio; Figure 8) and low sterane/hopane ratios (C_{29}-sterane/C_{30}-hopane) (Table 6) suggest a possible lacustrine depositional environment for the source rock organic matter. Therefore, the Mamfe Formation source rock facies were deposited in an anoxic-bottom lake. [39] and [40] reported that gammacerane is an indicator of salinity stratified water column; it is present in all of the samples analysed. This suggests that there was a salinity-stratified water column and sub-oxic bottom water conditions at the time of accumulation of the Mamfe Formation sediments. This also confirm the works of [41] and [42] indicating the occurrence of salt spring in the basin. The land plant-derived biological marker, 18α (H)-oleanane, is presence in all of the analysed samples. This supports the interpretation of substantial terrestrial-sourced organic matter input in the sediments according to [7] and [8]. The C_{24}/C_{23} and C_{22}/C_{21} tricyclic terpane values (Table 4) are low in the studied samples and are interpreted as indicating marine and terrigenous organic matter origin.

The cross-plots of C_{24} tetracyclic terpane/C_{26} tricyclic terpane vs. tricyclic terpane C_{26}/C_{25} (Figure 9) and C_{24} tetracyclic terpane/C_{26}(R+S) tricyclic terpane vs. tricyclic terpane C_{23}/C_{24} (Figure 10) further support increased terrigenous organic matter input.

[43] have reported that a dominance of C_{27} steranes indicates a predominance of marine phytoplankton, whereas a dominance of C_{29} steranes would indicate a strong terrestrial contribution and C_{28} steranes might indicate a substantial contribution by lacustrine algae. A particularly high abundance of C_{29} sterane (relative to C_{27}–

C_{28} steranes) is present in the analysed studied samples. The cross-plots of Pr/Ph ratios vs. Sterane/hopane (Figure 11) and Pr/Ph ratios vs. sterane $C_{27}/(C_{27}+C_{29})$ ratios (Figure 12) further confirm that the organic matter in the studied samples is of terrestrial origin with minor marine and lacustrine influences. The regular-sterane ternary diagram indicates that the organic matter in the studied samples of the Mamfe Formation were deposited mainly in an open marine environment (Figure 13 and Figure 14). A high steranes/hopanes ratio (> 1) represent a strong input of marine organic matter and in particular of planktonic algae while low ratios of steranes/hopanes (<1) are attributed to the abundant terrigenous organic matter input [44]. The steranes/hopanes ratio of the studied Mamfe extract are generally less than one (Table 6), implying a terrigenous organic matter source input.

5.2. Source Rock Maturity based on *n*-alkane and Biomarker Parameters

In this study, *n*-alkane and biomarker maturity parameters were used to assess the thermal maturity of organic matter within the sediments. CPI or OEP values of >1.0 or < 1.0 indicate thermal immaturity, and values of 1.0 indicate that the organic matter is thermally mature [7] The relatively high concentrations of light *n*-alkanes, high CPI, and odd-over-even predominance (OEP) values of 1.0 suggest that the studied samples are thermally mature (Figure 15). The relationship between isoprenoid Pr/*n*-C_{17} and Ph/*n*-C_{18} ratios (Figure 7) also shows that all analysed samples are thermally mature. The Ts/ (Ts + Tm) ratio which dependent on thermal maturity and origin of organic matter [7] indicates that sediments are early mature to mature level of thermal maturity. The Mamfe samples have a moretane/hopane (M/H) ratio in the range of 0.16 to 0.27, suggesting that the samples are thermally mature. Overall, the biomarker thermal maturity parameters indicate that all analysed Mamfe samples are, at least, mature, and are likely approaching oil-window maturity. This supports vitrinite reflectance (%Ro) measurements, which range from 0.55 to 0.82 %Ro as reported by [2]. The C_{29} ββ/(ββ + αα) and 20S/ (20S + 20R) sterane ratios were also used for the assessment of organic maturation in the sediments. These ratios are directly proportional to thermal maturity and suggest that most of the organic matters within the studied sediments are within the oil window [7,8]. The cross-plot of two the biomarker maturity parameters (Figure 16) further indicates that the studied samples are thermally matures.

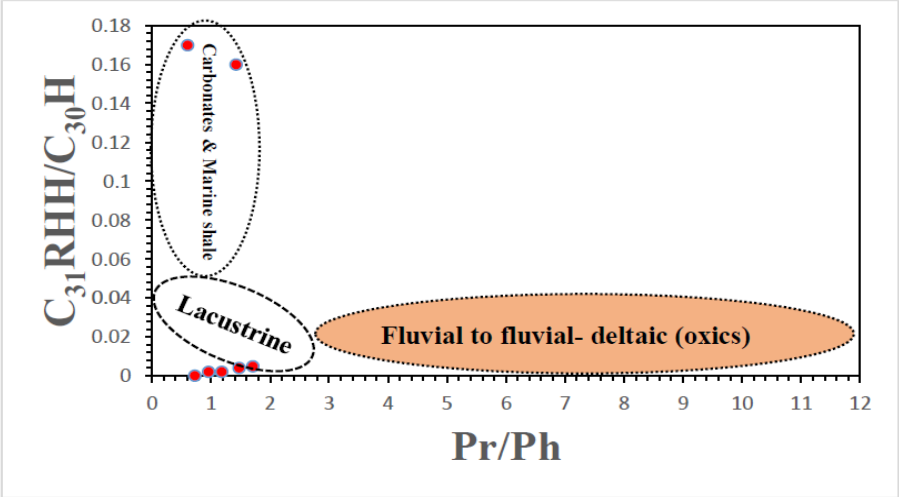

Figure 8. Hopane and isoprenoid ratios of organic matter extracts used to discriminate the depositional environments for Mamfe sediments (modified after 8)

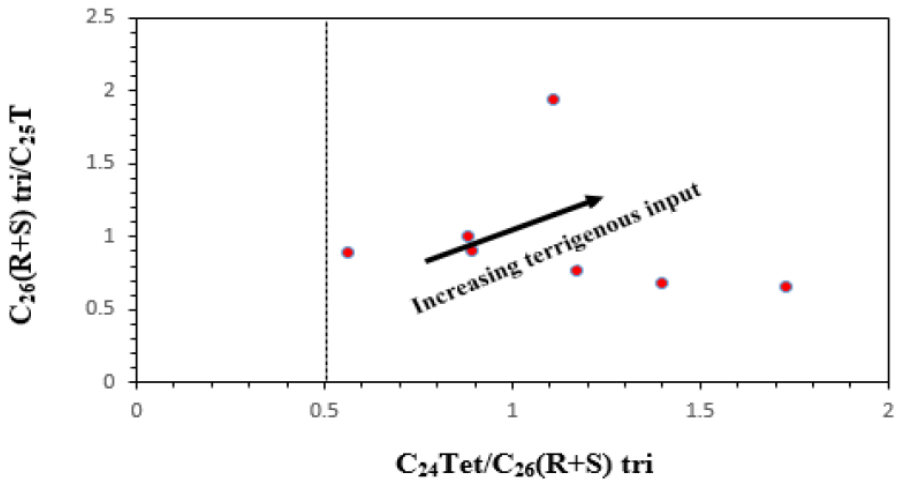

Figure 9. Cross-plot of C_{26} (R+S) T/C_{25}T versus C_{24}Tet/C_{26}(R+S) T showing increasing terrigenous input in the studied sediments (after 30)

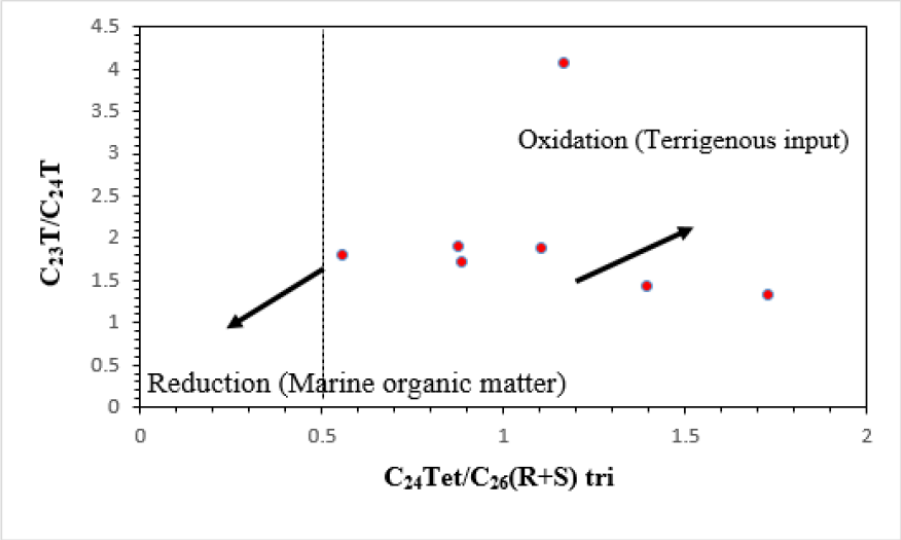

Figure 10. Cross-plot of $C_{23}T/C_{24}T$ versus $C_{24}Tet/C_{26}T$, also showing increasing terrigenous input in the studied samples (after 30)

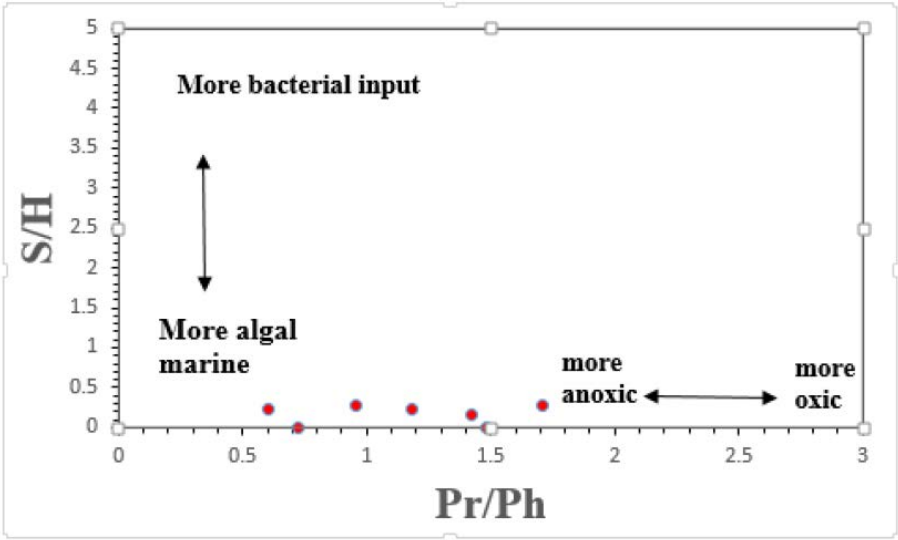

Figure 11. Cross-plot of hopane/sterane ratios vs. Pr/Ph ratios (after 30)

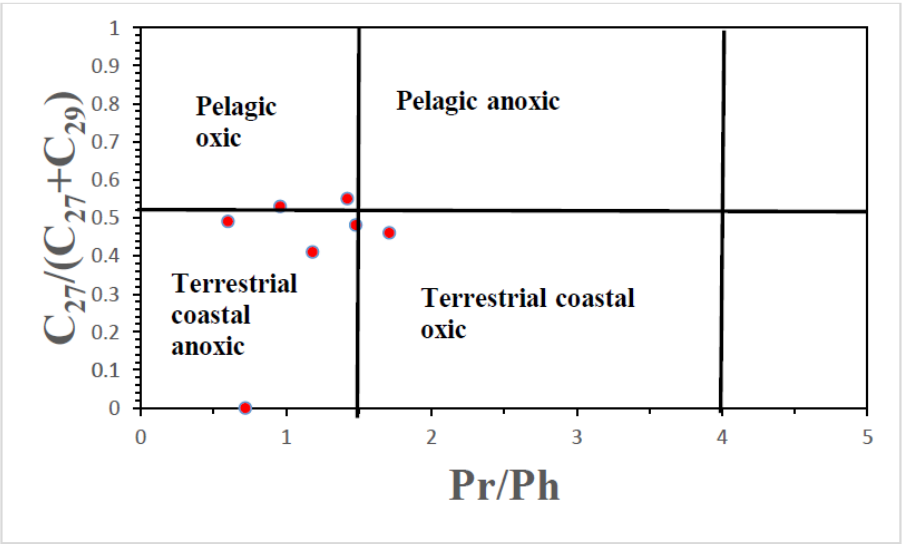

Figure 12. Cross-plot of $C_{27}/ (C_{27}+ C_{29})$ regular steranes versus Pr/Ph ratios showing paleodepositional conditions and source origin of the organic matter extracts of the studied sediments

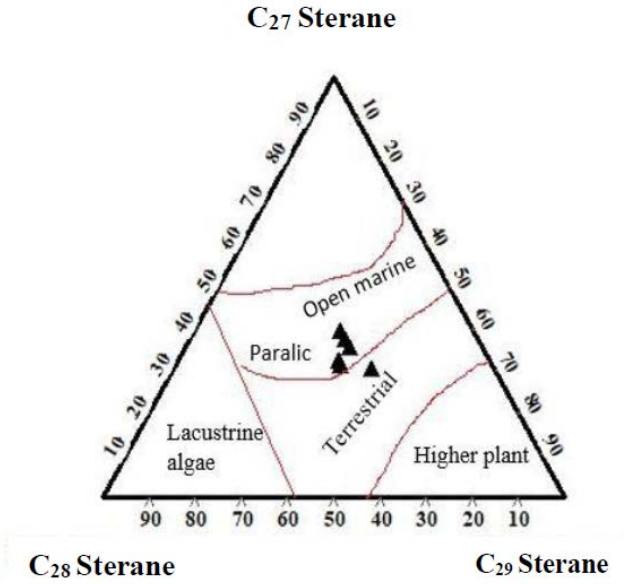

Figure 13. Ternary plot showing the relationship between sterane composition and depositional environment (after 43)

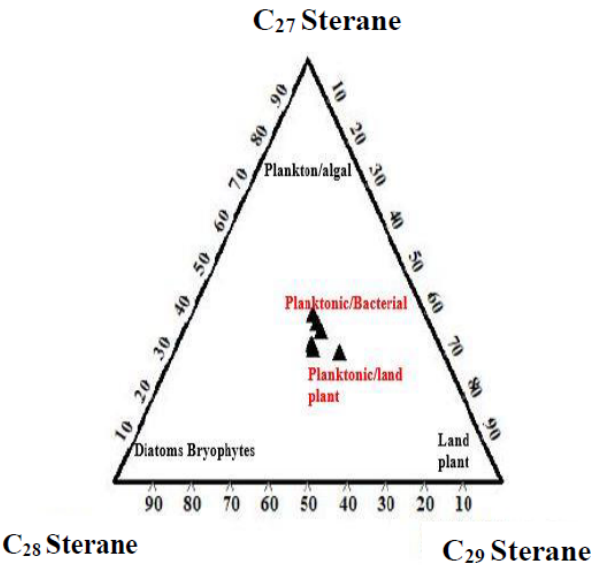

Figure 14. Relationship between regular sterane compositions, organic matter origin, and depositional environment for the analysed Mamfe extracts (modified after 43)

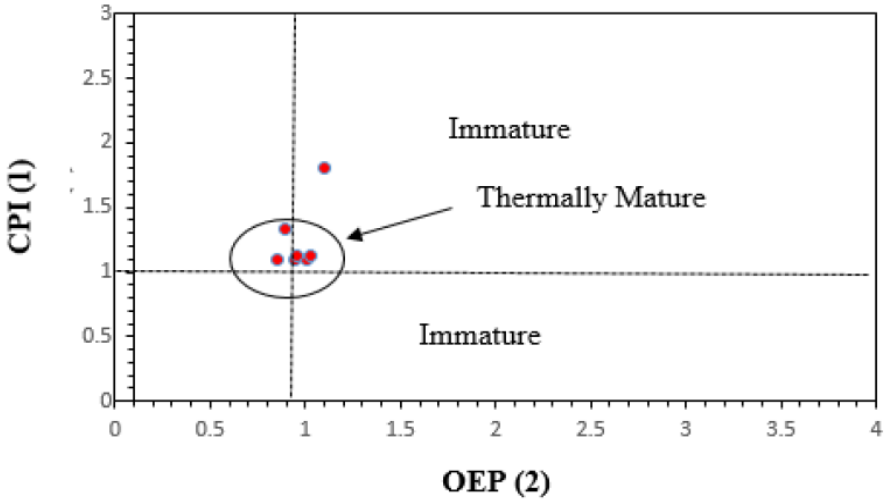

Figure 15. Plots of *n*-alkanes showing interpretation of organic matter thermal maturity in the studied samples

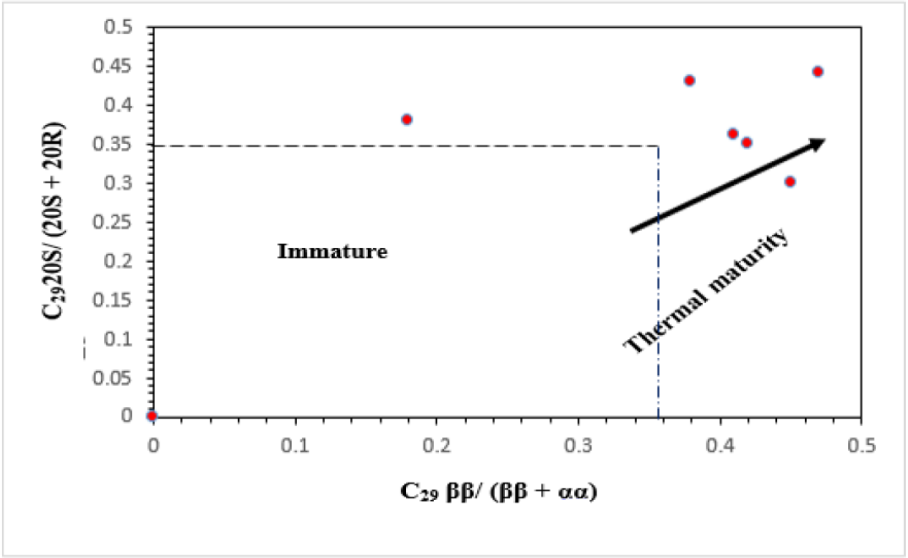

Figure 16. Cross-plot of two biomarker parameters sensitive to thermal maturity for the studied samples, which shows that most of the Mamfe Formation samples plot in the area of early oil window maturity (after 7)

6. Conclusions

Biomarker geochemical characterization of the Cretaceous organic-rich shales from the Mamfe Formation, Mamfe Basin was carried out to determine organic matter source input, paleo-environmental conditions, thermal maturity and hydrocarbon generation potential. Organic matter source input characterization, based on reliable observations from *m/z* 85, *m/z* 191, and *m/z* 217 distributions, suggests a land plant origin for the organic matter with lacustrine and marine influences. However, the waxiness index, terrigenous/aquatic ratios, and oleanane index support a predominance of terrigenous organic matter origin in the sediments. Biomarker maturation parameters and *n*-alkane data including Ts/(Ts + Tm), moretane/hopane , 20S/(20S + 20R), and ββ/(ββ + αα) C_{29} sterane ratios along with CPI and OED indicate that the analysed samples from Mamfe Formation sit at mature oil window generation. Biomarker characteristics suggest deposition in a highly saline reducing environment.

Acknowledgements

The first author will like to appreciate Pan African University especially the Institute of Life and Earth Sciences (Including Health and Agriculture) –University of Ibadan, Ibadan, Nigeria for providing the platform for this work to be done. The authors are also grateful to the learned reviewers for their valuable suggestions and comments which have greatly improved the manuscripts.

References

[1] Eseme, E., Littke, R., and Agyingi, C. M., (2006). Geochemical characterization of a Cretaceous black shale from the Mamfe Basin, Cameroon. Petroleum Geoscience, v.12, p. 69-74.

[2] Ndip E. A., Christopher M. A., Mathew E.N., James C.H., and Michael A.O., (2019). Organic Petrography and Petroleum source rock evaluation of the Cretaceous Mamfe Formation, Mamfe Basin, Southwest, Cameroon Inter. J Coal Geology 202: 27-37.

[3] Reyment, R. A., (1954).The stratigraphy of the Southern Cameroons. Geologiska FöreningensI Stockholm Förhandlingar, v. 76, p. 661-683.

[4] Reyment, R. A., (1965). Aspects of the geology of Nigeria. Ibadan University press, Ibadan, 145pp

[5] Abolo, M. G. (2008). Geology and petroleum potential of the Mamfe Basin, Cameroon, Central Africa, Africa Geoscience Review. Special Publication, v. 1 and 2, p. 65-77.

[6] Eyong, J. T., (2003). Litho - Biostratigraphy of the Mamfe Cretaceous Basin, S.W. Province of Cameroon – West Africa. Ph.D. thesis, University of Leeds, 265 pp.

[7] Peters K.E., and Moldowan J.M. (1993).The biomarker guide: interpreting molecular fossils in petroleum and ancient sediments. Prentice Hall, Inc, Englewood Cliffs, New Jersey

[8] Peters K.E., Walters C.C., and Moldowan J.M. (2005). The biomarker guide: biomarkers and isotopes in petroleum exploration and earth history, second ed, vol 2. Cambridge University Press, Cambridge

[9] Hakimi M.H., Wan Hasiah A., Shalaby M.R. (2011).Organic geochemical characteristics and depositional environments of the Jurassic shales in the Masila Basin of Eastern Yemen. Geo Arabia 16: 47-64.

[10] Hakimi M.H., Abdullah W.H., Shalaby M.R (2012).Molecular composition and organic petrographic characterization of Madbi source rocks from the Kharir Oilfield of the Masila Basin (Yemen): palaeoenvironmental and maturity interpretation. Arab J Geosci 5: 817-831.

[11] Burton, Z. F. M., Moldowan, J. M., Sykes, R., Graham, S. A. (2018). Unravelling petroleum degradation, maturity, and mixing and addressing impact on petroleum prospectivity: insights from frontier exploration regions in New Zealand. Energy & Fuels, 32(2), 1287- 1296.

[12] Burton, Z. F., Moldowan, J. M., Magoon, L. B., Sykes, R., & Graham, S. A. (2019). Interpretation of source rock depositional environment and age from seep oil, east coast of New Zealand. International Journal of Earth Sciences, 1-13.

[13] Petters, S. W., (1978). Stratigraphic evolution of the Benue Trough and its implications for the Upper Cretaceous paleogeography of West Africa. Journal of Geology, v. 86, p. 311-322.

[14] Benkhelil, J., (1989).The origin and evolution of the Cretaceous Benue Trough (Nigeria Journal of African Earth Sciences, v. 8, p. 251-2824.

[15] Fairhead, J.D., and Green, C.M., (1989). Controls on rifting in Africa and the regional tectonic model for the Nigeria and East Niger rift basins. Journal of African Earth Sciences 8 (2/3/4), 231-249.

[16] Bassey, C. E., Eminue, O. O., and Ajonina, H. N., (2013). Stratigraphy and deposition environments of the Mamfe Formation and its implication on the tectonosedimentaryevolution of the Ikom-Mamfe Embayment, West Africa. *Central European Journal*.

[17] Eyong, J. T., Wignall, P., Fantong, W. Y., Best, J., Hell, J. V., (2013).Paragenetic sequences of carbonate and sulphide minerals of the Mamfe Basin (Cameroon): Indicators of palaeofluids, palaeo- oxygen levels and diagenetic zones. Journal of African Earth Sciences, v.86, p. 25-44.

[18] Dumort, J.C. (1968).Carte Géologique de reconnaissance a 1/500000 avec notice explicative. Feuille Douala-Quest. Direction des Mines et de Géologie, Cameroun.

[19] Wilson, R.C., 1928. Notes on the geology of the Mamfe Division, Cameroon Province. Geological Survey of Nigeria Occasional Paper 6.

[20] Ndip E.A., Agyingi, C.M., Nton, M.E., Oladunjoye, M.A., (2018). Review of the geology of Mamfe. Sedimentary basin, SW Cameroon, Central Africa. J. Oil, Gas Petrochem. Sci.

[21] Tissot, B.P., Welte, D.H., (1984). Petroleum Formation and Occurrence, 2ndedn.springer, New Berlin, Heidelberg, New York, Tokyo.

[22] Peters K.E., and Cassa, M.R., (1994). Applied source rock Geochemistry. In: L.B.Magoon, and W.G.Dow, eds., The Petroleum system- From source to trap, APPG Memoir 60,Tulsa, Oklahoma, p.93-117.

[23] Espitalié, J., Deroo G., and Marquis F., (1985). Rock-Eval pyrolysis and its applications. Second part. Review of the French Institute of Petroleum 40 (6),755-784.

[24] Hunt J.M., (1996). Petroleum, Geochemistry and Geology 2nd edition. W.H. Freeman Company, New York (744p).

[25] Bray E.E. and Evans E.D. (1961).Distribution of n-paraffins as a clue to recognition of source beds.Geochim Cosmochim Acta 22: 2-15.

[26] Leythaeuser D., and Welte D. H. (1969). Relation between distribution of heavy n-paraffins and coalification in carboniferous coals from saar District, Germany.In Advances in Organic Geochemistry 1968(Edited by Schenk P.A. and Havenaar J.),pp 429-442.Pergamon Press, Oxford.

[27] Meyers P.A., and Snowdon LR (1993). Types and maturity of organic matter accumulated during Early Cretaceous subsidence of the Ex-mouth Plateau, Northwest Australia margin. AAPG Stud Geol 37: 119-130.

[28] Scalan R.S. and Smith JE (1970).An improved measure of the odd-even predominance in the normal alkanes of sediment extracts and petroleum. Geochim Cosmochim Acta 34: 611-620.

[29] Hakimi M.H, and Abdullah W.H. (2013). Organic geochemical characteristics and oil generating potential of the Upper Jurassic Safer shale sediments in the Marib-Shabowah Basin, western Yemen. Org Geochem 54:115-124.

[30] El Diasty and Moldowan, (2013).The western desert versus Nile Delta: a comparatives molecular biomarker study. Marine and Petroleum Geology.v.46, p 319-334.

[31] Gülbay R.K., Kırmacı M.Z, Korkmaz S. (2012). Organic geochemistry and depositional environment of the Aptian bituminous limestone in the Kale Gümüshane area (NETurkey):

an example of lacustrine deposits on the platform carbonate sequence. Org Geochem 49: 6-17.

[32] Adegoke, A.K., Sarki Yandoka, B.M., Abdullah, W.H., Akaegbobi I.M., (2014). Molecular geochemical evaluation of Late Cretaceous sediments from Chad (Bornu) Basin, NE Nigeria: implication for paleodepositional conditions, source input and thermal maturation. Arab J Geosci 8, 1591-014-1341.

[33] Powell TG, and McKirdy DM (1973). Relationship between ratio of pristine to phytane, crude oil composition and geological environment in Australia. Nature 243: 37-39.

[34] Didyk B.M., Simoneit B.R.T, Brassell S.C., Eglinton G. (1978). Organic geochemical indicators of palaeoenvironmental conditions of sedimentation. Nature 272: 216-222.

[35] Ten Haven HL, de Leeuw JW, Rullkötter J, Sinninghe Damsté JS (1987).Restricted utility of the Pristine /phytane ratio as a palaeoenvironmental indicator. Nature 330:641-643.

[36] Vu TTA, Zink KG, Mangelsdorf K, Sykes R, Wilkes H, Horsfield B (2009). Changes in bulk properties and molecular compositions within New Zealand Coal Band solvent extracts from early diagenetic to catagenetic maturity levels. Org Geochem 40: 963-977.

[37] Waples D.W. and Machihara T (1991). Biomarkers for Geologists: a practical guide to the application of steranes and triterpanes in petroleum geology. American Association of Petroleum Geologists Methods in Exploration 9, Tulsa, Oklahoma.

[38] Obermajer M, Fowler MG, and Snowdon LR (1999). Depositional environment and oil generation in Ordovician source rocks from southwestern Ontario, Canada: organic geochemical and petrological approach. Am Assoc Pet Geol Bull 83:1426-1453.

[39] Sinninghe Damsté JS, Kenig F, Koopmans MP, Koster J, Schouten S, Hayes JM, de Leeuw JW (1995). Evidence for gammacerane as an indicator of water column stratification. Geochim CosmochimActa 59:1895-1900.

[40] Ten Haven HL, de Leeuw JW, Rullkötter J, SinninghеDamsté JS, Scheck PA, Palmer SE, Zumberge JE, Fleet AJ, Kelts K, Talbot MR, Fleet AJ, Kelts K, Talbot MR (1988).Application of biological markers in the recognition of palaeo-hypersaline environments. In: Fleet AJ, Kelts K, Talbot MR (eds) Lacustrine Petroleum Source Rocks.

[41] Tanyileke G.Z., (1994). Geochemistry of the CO_2 rich and lake and soda spring along the Cameroun Volcanic line, Cameroun. Ph-D, Okoyama Univ., 155p.

[42] Eseme, E., Agyingi, C. M., and Foba-Tendo J., (2002). Geochemistry and genesis of brine emanations from Cretaceous strata of the Mamfe Basin, Cameroon. Journal of African Earth Sciences, v.35,p. 467-476.

[43] Huang W.Y. and Meinschein W.G. (1979). Sterols as ecological indicators. Geochim Cosmochim Acta 43:739-745.

[44] French K.L., Sepúlveda, J., Trabucho-Alexandre, J., Gröcke, D.R., and Summons, R.E. (2014).Organic geochemistry of the early Toarcian oceanic anoxic event in Hawsker Bottoms, Yorkshire, England. Earth and Planetary Science Letters 390, 116-127.